Overview and Evaluation of a Computational Bone Physiology Modeling Toolchain and Its Application to Testing of Exercise Countermeasures

A. Schepelmann[1], J. A. Pennline[2], C. R. Werner[1], K. M. Gilkey[2], and B. E. Lewandowski[2]

[1] ZIN Technologies, Inc., 6745 Engel Road, Airport Executive Park, Cleveland, OH 44130
[2] NASA Glenn Research Center, 21000 Brookpark Road, Cleveland, OH 44135

INTRODUCTION

Prolonged microgravity exposure disrupts natural bone remodeling processes and can lead to a significant loss of bone strength, increasing injury risk during missions and placing astronauts at a greater risk of bone fracture later in life. Resistance-based exercise during missions is used to combat bone loss, but current exercise countermeasures do not completely mitigate the effects of microgravity. To address this concern, we are working to develop a personalizable, site-specific computational modeling toolchain of bone remodeling dynamics to understand and estimate changes in volumetric bone mineral density (vBMD) in response to microgravity-induced bone unloading and in-flight exercise.

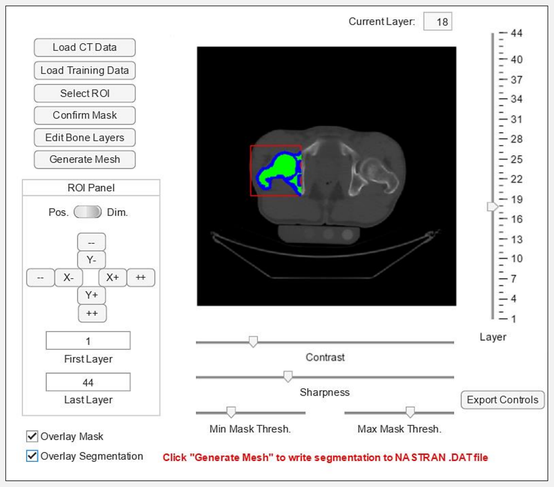

Figure 1: FE generation GUI and probabilistic classification results. Red: User-specified ROI. Blue: Identified cortical bone. Green: Identified trabecular bone.

FINITE ELEMENT MODEL GENERATION

Personalized finite element (FE) bone models are procedurally generated by combining user-guided pre- and post-processing steps with a probabilistic classification scheme to identify bone containing pixels in input Digital Imaging and Communications in Medicine Computed Tomography (DICOM CT) image stacks.

Classification is performed on a three dimensional user-specified image region of interest (ROI), whose size and position can be modified using buttons in a graphical user interface (GUI) (Fig. 1). Classification can be further constrained by selecting groups of pixels within this ROI using a binary mask, whose limits can be adjusted via sliders in the GUI. This mask is then processed using an image morphology heuristic to ensure continuity of pixels within the mask.

Masked pixels are segmented into three classes (cortical bone, trabecular bone, and other) using a Gaussian Naïve Bayes classifier [1]. This classifier uses Bayes' theorem to determine what class $Y = y_j$ a sample most likely belongs to based on a vector of features $\boldsymbol{X} = \boldsymbol{X_i} =< x_1, x_2, \dots, x_n >$, and takes the form

$$P(Y = y_j | \boldsymbol{X} = \boldsymbol{X_i}) = \frac{P(\boldsymbol{X} = \boldsymbol{X_i} | Y = y_j) P(Y = y_j)}{P(\boldsymbol{X} = \boldsymbol{X_i})}$$

Each feature in $\boldsymbol{X}$ is "naïvely" assumed to be conditionally independent of other features, allowing the conditional probability model to be rewritten as

$$P(\boldsymbol{X} = \boldsymbol{X_i} | Y = y_j) = \prod_{k=1}^{n} P(\boldsymbol{X_i}(k) = x_k | Y = y_j)$$

After computing the relative likelihood that a pixel belongs to each class, it is assigned a label using the rule

$$Y^{new} \leftarrow \arg\max_{y_j} P(y = y_j) \prod_{k=1}^{n} P(\boldsymbol{X_i}(k) = x_k | Y = y_j)$$

After classification, a post-processing heuristic is applied to labeled pixels to ensure that their locations are physiologically feasible and that they will generate a continuous two-material FE model. After optional user-guided post-processing, a standalone NASTRAN FE model is then generated from the segmentation, whose material properties are initialized from CT scan pixel intensities using the method described in [2].

COMPUTATIONAL BONE REMODELING MODEL

The computational bone model simulates bone remodeling dynamics to capture bone loss trends in microgravity. Specifically, the model is designed to understand and estimate site-specific changes in vBMD in response to microgravity-induced bone unloading and in-flight exercise, which in turn affects bone material properties and bone strength. The model involves three major bioscience areas: removal and replacement of bone packets via the bone remodeling process, mechanotransduction, and cellular dynamics physiology. Cellular dynamics are described via state variables that drive bone resorption and formation rates of change (ROCs) through a set of coupled differential equations (Fig. 2). These rates are influenced by loads applied to the bone through a mechanostransduction model (Fig. 3), which couples FE simulations that model in-flight exercise with the cellular dynamics model to form the computational bone remodeling model. A schematic of this model is shown in Figure 4.

	State Variables	Driving Process	Dependencies
BVF ROCs	Mineralized VF Osteoid VF	Removal & Replacement of Bone Packets (Remodeling Units)	Activation Density Bone Remodeling Units BRU Area Resorbed BRU Area Formed Active Resorbing Cell Pop. Active Forming Cell Pop.
Cell Population ROCs	Active Osteoblasts Active Osteoclasts Responding Osteoblasts	RANK-RANKL-OPG Pathway	Transforming Growth Factor Parathyroid Hormone RANKL Osteoprotegerin Hormone PGE_2 Nitric Oxide

Figure 2: Computational bone remodeling model state variables.

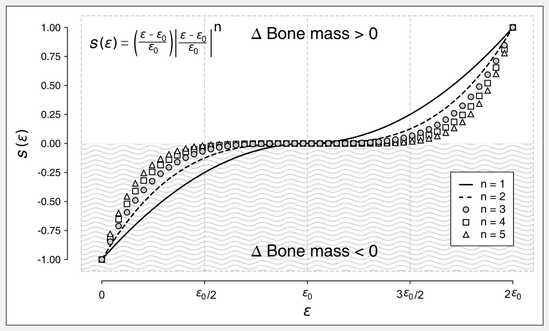

Figure 3: Mechanostat model.

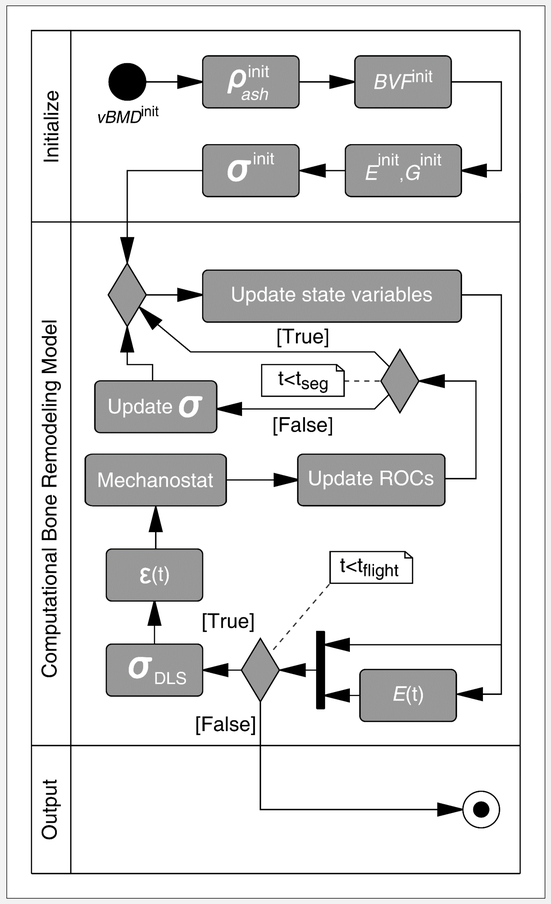

Figure 4: Computational bone remodeling model schematic.

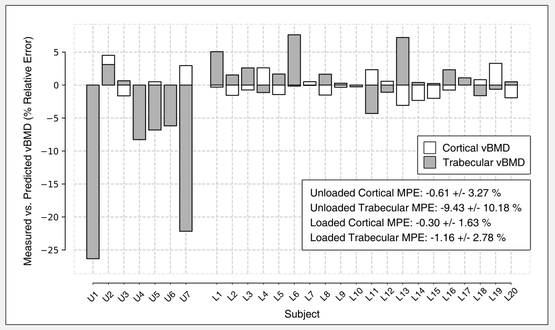

Figure 7: vBMD relative error for unloaded and loaded remodeling simulations.

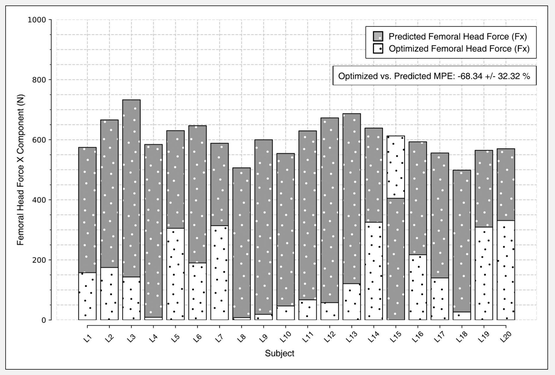

Figure 8: Predicted and optimized femoral head force to achieve post-study vBMD values of exercising subjects.

METHODS

The toolchain is evaluated against data from a 70-day head-down-tilt bed rest study by assessing the model's ability to predict post-study cortical and trabecular vBMD of participants who did and did not perform exercise [3]. Exercises performed during the study were consistent with NASA's iRAT regimen, an exercise protocol designed to maintain vBMD during spaceflight. For analysis, the net effect of this protocol is modeled as a single daily load stimulus (DLS) exercise needed to maintain bone health – walking 5,000 steps per day at a speed of 5 km/h – whose net stress S is

$$S = \sum_{j=1}^{n} \ln(1 + N_j)\bar{\sigma}_j f_j$$

where N_j is the number of repetitions of exercise j performed with a frequency f_j and $\bar{\sigma}_j$ is the mean exercise stress. To account for subject anthropometry, which affects force magnitudes during walking, regression curves were generated from publicly available data to estimate femoral head and greater trochanter forces based on subject mass, stride length, and walking speed (Fig. 5) [4]. FE analysis is used to simulate exercise-induced bone loading. Forces are applied to a representative FE model of the femur generated using the method described previously (Fig. 6). The model's predictive ability was assessed by comparing the regression-derived maintenance force to a force F optimized as

$$J(F) = \alpha(\rho^{cort}_{QCT,sim} - \rho^{cort}_{QCT,meas})^2 + (1 - \alpha)(\rho^{trab}_{QCT,sim} - \rho^{trab}_{QCT,meas})^2$$

where $\rho^{cort}_{QCT,sim}$, $\rho^{trab}_{QCT,sim}$, $\rho^{cort}_{QCT,meas}$, and $\rho^{trab}_{QCT,meas}$ are the simulated and measured post-study vBMDs, and α is the ratio of cortical elements to the total number of elements in the representative two-material FE model of the femur.

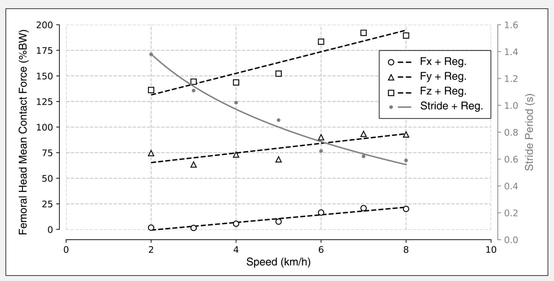

Figure 5: Femoral head joint force and stride period regression curves for estimating loading and DLS parameters.

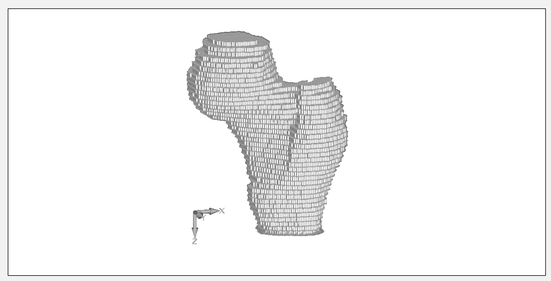

Figure 6: Programmatically generated femur finite element model used for force optimizations.

RESULTS AND DISCUSSION

The developed toolchain provides insight into the amount of exercise stimulus needed to minimize bone loss, and can create subject-specific bone models that are potentially useful for quantifying the amount of exercise stimulus needed to mitigate vBMD decline during spaceflight.

Specifically, the computational bone model is able to predict post-study cortical and trabecular vBMD of control subjects who did not perform exercise with a mean percent error (MPE) of -0.61± 3.27% and -9.43 ± 10.18%, respectively. For subjects who performed exercise, post-study vBMD values predicted using the toolchain show convergence during optimization, achieving cortical and trabecular MPEs of -0.30 ± 1.63% and -1.16 ± 2.73%, respectively, though optimized forces were lower than regression-predicted maintenance forces for the majority of subjects. While all optimized forces were greater than zero, indicating that the model captures the effects of performing exercise, the MPE between optimized and regression-predicted forces is -68.34 ± 32.32%.

The discrepancy between regression-predicted and optimized forces could result from several sources. First, while vBMD values converged during optimization, cortical and trabecular values are not directly coupled. In cases where the optimized force were near zero, the optimization favored one quantity over another, and therefore likely terminated at a local minimum. This adversely affected the final value of the optimized force. To address this issue, we plan to conduct further studies that couple cortical and trabecular vBMD densities by first converting these quantities to a single bone densitometry (DXA) value. Next, regression equations used to predict forces on the femur during walking were based on data from a single subject. As a result, forces predicted by the regression may be artificially high. Data from additional subjects will need to be incorporated into the regression to investigate this phenomenon. Finally, all data was analyzed using a representative FE model and the same computational bone model parameters for each subject. To address this issue, subject-specific CT data and additional work to investigate how model parameters are affected by subject-specific body anthropometry are necessary.

REFERENCES & ACKNOWLEDGMENTS

[1] Mitchell, T. M. (1997). Machine Learning. McGraw-Hill, Inc., New York, NY, USA, 1st edition.
[2] Keyak, J. H. et al. (2005). Predicting proximal femoral strength using structural engineering models. Clinical Orthopaedics and Related Research, 437:219-228.
[3] Taibbi, G. et al. (2016). Ocular outcomes comparison between 14- and 70-day head-down-tilt bed rest. Investigative Ophthalmology and Visual Science, 57(2):495-501.
[4] Bergman, G. (2008) Orthoload. Charité Universitätsmedizin Berlin, http://www.orthoload.com

The authors thank Lealem Mulugeta, Aaron Godfrey, and Abhishektha Boppana for their assistance with this research.